Ultrafast Dynamics and Hydrogen−Bond Structure in Aqueous Solutions of Model Peptides

ARTICLE *in* THE JOURNAL OF PHYSICAL CHEMISTRY B · AUGUST 2010

Impact Factor: 3.3 · DOI: 10.1021/jp106423a · Source: PubMed

3 AUTHORS:

Kamila Mazur

14 PUBLICATIONS **162** CITATIONS

SEE PROFILE

Ismael A Heisler

University of East Anglia

48 PUBLICATIONS **539** CITATIONS

SEE PROFILE

Stephen R. Meech

University of East Anglia

154 PUBLICATIONS **3,598** CITATIONS

SEE PROFILE

Ultrafast Dynamics and Hydrogen-Bond Structure in Aqueous Solutions of Model Peptides

Kamila Mazur, Ismael A. Heisler, and Stephen R. Meech*

School of Chemistry, University of East Anglia Norwich NR4 7TJ, United Kingdom

Received: July 12, 2010

The dynamics of water molecules in the hydration layers of proteins are critical for biological function. Here the molecular dynamics in aqueous solutions of model hydrophilic and amphiphilic dipeptides are studied as a function of concentration using the ultrafast optical Kerr effect (OKE). The OKE is a direct time-domain method which yields both picosecond time scale molecular dynamics and low-frequency (Terahertz) Raman spectra, which contain information on the hydrogen-bonded structure of aqueous solutions. Two distinct concentration regimes are identified, above and below 0.4 M peptide concentration. In the low-concentration regime the tetrahedral water structure is largely preserved but the structural dynamics in water are slowed significantly by interaction with the peptide. The slow down is more marked for the hydrophilic than the amphiphilic peptide. Suppression of water structural dynamics observed is greater than that reported for retardation of the water reorientation in NMR, reflecting the different dynamics probed by these different methods. Above 0.4 M the tetrahedral water structure is more strongly perturbed, a contribution to the THz Raman spectrum from the solvated peptide is observed, and structural dynamics in the solution are markedly slowed. This is assigned to slow relaxation within an H-bonded network of peptide molecules. The strong concentration dependence observed goes some way toward explaining disagreements between different measurements of the dynamics of peptide solvation which have appeared in the literature.

Introduction

Water plays a key role in the structure and dynamics of a wide range of biological processes. Spatially fixed 'structural' water molecules are an integral part of the structure of proteins,[1] while more mobile interfacial water is critical to protein folding and membrane stability.[2,3] An understanding of the nature of these solvating water layers is thus of central importance to understanding biological function.[4,5] The hydration layer must interact sufficiently strongly with its associated 'solute' (protein, membrane, etc.) to stabilize it in the appropriate environment but not so strongly as to block surface sites or inhibit structural change, thus adding to the activation free energy associated with a particular function. The evident importance of and the subtle interplay between, water and biological interfaces have led to a number of detailed investigations of the structure, range, and dynamics of the solvation layer.[1−20] These have involved a diverse range of experimental and theoretical methods, and each has provided important new insights. However, there remain significant elements of disagreement and controversy, particularly regarding the dynamics of water molecules within the solvation layer.[8]

The range of possible solvated interfaces within any given cell is vast. In an effort to provide some generic model data a number of studies have been conducted on the solvation of relatively simple model peptides in aqueous solution.[10−20] The pair of dipeptides *N*-acetyl-glycine-methylamide (NAGMA) and *N*-acetyl-leucine-methylamide (NALMA) have been especially widely studied, as they have similar sizes but NAGMA is hydrophilic while NALMA is amphiphilic due to its hydrophobic leucine side chain. Experimental methods applied to these samples have included neutron scattering,[15−18] NMR relaxation,[10,19] dielectric relaxation,[20] and terahertz absorption spectroscopy.[11] These experimental studies have recently been complemented by detailed molecular dynamics simulations.[13,21]

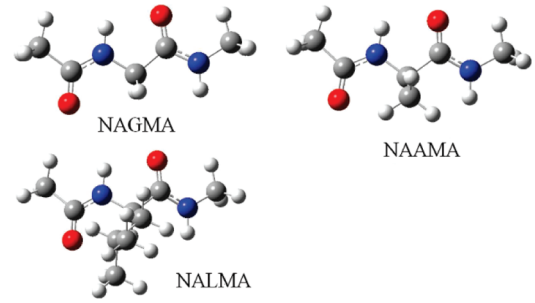

Figure 1. Structures of the three peptides studied: NAGMA, NAAMA, and NALMA.

There is broad agreement among these diverse experiments that a population of water molecules exists in solutions of NAGMA and NALMA at around 295 K which relaxes on a time scale roughly twice as long as that found in pure water. There is however a significant area of disagreement concerning the existence of a more slowly relaxing population. No such population is observed in NMR experiments.[19] In contrast, in neutron scattering the existence of 'slow' water (relaxation time >13 ps) is inferred from measurements of the elastic incoherent structure factor.[17] Similarly, dielectric relaxation experiments recover relaxation dynamics on the time scale of tens of picoseconds, and a component as long as hundreds of picoseconds has been reported.[20] To provide a new perspective on these important systems we report here the dynamics of aqueous solutions of the three dipeptides NAGMA, NALMA, and NAAMA (*N*-acetyl-alanine-methylamide) (Figure 1) as a function of concentration between 0.1 and 3 M using the ultrafast optically heterodyne-detected-optical Kerr effect (OHD-OKE).[22,23]

The OHD-OKE offers two distinct advantages compared to methods previously applied to the study of solvated peptide

* To whom correspondence should be addressed. E-mail: s.meech@uea.ac.uk.

10.1021/jp106423a
Published on Web 07/29/2010

dynamics. First, it is a direct time-domain measurement, so the analysis of the transient response is in the first instance model independent. This distinguishes it from neutron scattering and dielectric relaxation measurements, in which the dynamical information is usually extracted from an assumed line shape. Such line shapes are in general well founded, but ambiguities can arise in the case of heterogeneous solutions, such as those presented by proteins and model peptides. Further, as a real-time method OHD-OKE avoids the temporal averaging that occurs in NMR measurements, which requires the assumption of a two-state model that has to be justified in a separate analysis (such as through the concentration dependence[19]). Second, the experiment provides a direct indication of the hydrogen-bonding (H-bonding) structure in the aqueous solution, because it measures (in the time domain) the THz depolarized Raman spectral density (RSD). The THz spectral density has been described previously for bulk water samples and found to be a sensitive probe of the water H-bonding network, in particular the degree of tetrahedral structure.[24−26] Thus, this unique ability of OHD-OKE to directly record in a single measurement the H-bond structure and the solution dynamics is potentially a very powerful one in developing a microscopic view of dynamics in hydration layers.

On the other hand, the OHD-OKE method has the disadvantage that it is not a proton-specific measurement (unlike neutron scattering and NMR) but, like dielectric relaxation, measures a susceptibility of the macroscopic sample (solvent plus solute). The OHD-OKE signal, $S(t)$, reflects the time-domain third-order response function $R(t)$ convoluted with the instrument response function (given by the second-order autocorrelation of the laser pulse, $G^{(2)}(t)$); $S(t) = R(t) \otimes G^{(2)}(t)$.[22,23] The $R(t)$ is in turn given by the time derivative of the polarizability correlation function of an off-diagonal element of the polarizability tensor, $\psi_{xz}(t)$[27]

$$R(t) = -\frac{1}{kT}\frac{\partial}{\partial t}\psi_{xz}(t)$$

Both single-molecule and intermolecular (interaction-induced) processes and their cross terms can contribute to the dynamics measured in $R(t)$. Progress in unravelling such complex multicomponent interactions can be made through a study of the composition dependence of the response (as described here). However, to obtain a detailed microscopic picture of the underlying dynamics, simulations of the polarizability correlation function are required.[27] OHD-OKE data for the simplest models of peptides (e.g., formamide) in water have already been reported.[28] Further, MD simulations for the dipeptide NALMA in aqueous solutions have recently been presented by Head-Gordon and co-workers.[13] Thus, OHD-OKE data coupled to MD simulations can provide very detailed insights into the structure and dynamics at water−peptide or water−protein interfaces.

In this work we report OKE studies of the three model peptides over a wide range of concentrations. The change in H-bond structure induced by the peptides is inferred from the THz Raman spectral density and becomes increasingly significant with increasing concentration. The concentration-dependent picosecond dynamics are associated with reorganization within the H-bonding network and at low concentrations can be assigned to the dynamics of bulk-like water perturbed by the solute. However, at higher concentration these dynamics are more complex and occur over a wide temporal range. This is associated with the formation of an H-bonded network of aggregated solvated peptide molecules. Specific modes associated with the solvated peptides are observed.

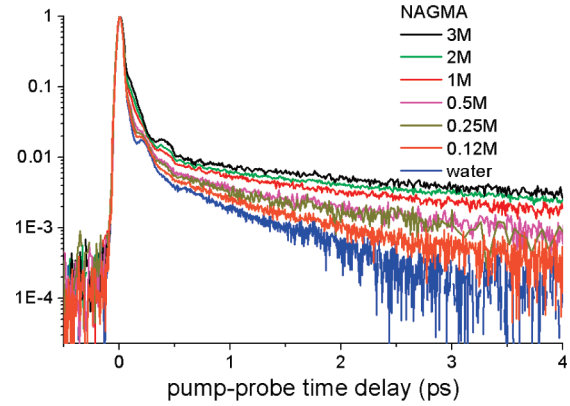

Figure 2. Short-time-window transient OHD-OKE data for NAGMA at different concentrations. Pure water is plotted for a comparison.

Experimental Section

The three peptides were obtained from Bachem (Germany) and used as received. They were dissolved in water at pH 4 and contained in 2 mm fused silica cells. All samples were filtered through a 0.20 μm Millipore filter to remove any particulate matter. Viscosities were measured in a separate experiment using a rotating conical plate rheometer. All measurements were made between 0.1 and 3 M (mol fraction 0.002−0.051) except for NALMA where maximum solubility was limited to 2 M.

The OHD-OKE measurement and its analysis are described in detail elsewhere.[22,23,29] The 800 nm, 30 fs, 300 mW output of a 68 MHz repetition rate home-built titanium sapphire laser was divided and routed through a conventional pump and probe geometry. The linearly polarized pump pulse induces a polarization in the sample at $t = 0$. The almost collinear probe pulse is overlapped with the pump pulse in the sample but polarized at 45° with respect to it. The probe is viewed through a polarizer oriented at −45°. The pump pulse induces a polarizability anisotropy in the initially isotropic sample, which results in depolarization of the probe, leading to partial probe transmission through the crossed polarizer, which is detected by a photodiode. As the pump−probe delay is increased the delay-dependent polarizability anisotropy relaxation is measured, reflecting the relaxation of the sample back to its initial isotropic state. Introduction of a heterodyne beam to interfere with the signal is straightforward and results in a dramatic improvement in signal to noise.[22,23,29] The signal can be analyzed either in the time domain or, through a Fourier transform (FT), in the frequency domain. Data in the frequency domain are also readily corrected for the finite bandwidth of the laser pulse.[22,23,29] It is straightforward to show that in this case the imaginary part of the frequency domain data are equivalent to the RSD, the Raman spectrum corrected for thermal occupation factors.[30]

Results and Discussion

The $S(t)$ data for NAGMA in water are shown in Figure 2 as a function of concentration on the 0−4 ps time scale; data for the other peptides were qualitatively similar, and measurements for the more slowly relaxing samples were extended to 30 ps (see Figure S1, Supporting Information). The traces are normalized to the intense narrow Gaussian feature centered at $t = 0$, which has a width reflecting the laser pulse and arises from the sample's instantaneous electronic response; as such it contains no information on molecular dynamics.[22,23] The responses at positive time reflect the nuclear dynamics in the solutions and

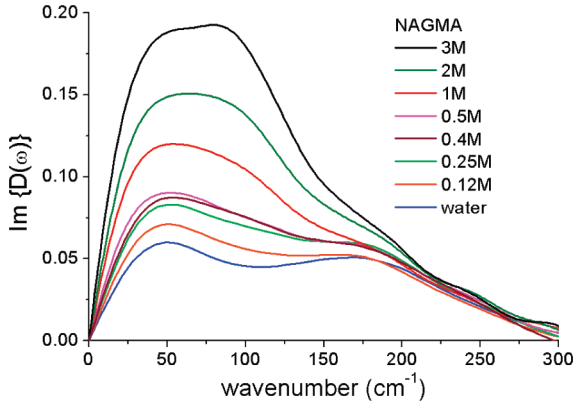

Figure 3. Im $D'(\omega)$ for NAGMA solutions. The Im $D'(\omega)$ of pure water (blue) is plotted as a reference. Weak oscillations seen in some of the data at higher wavenumber are an artifact of the Fourier transform and not reproducible or associated with any molecular features.

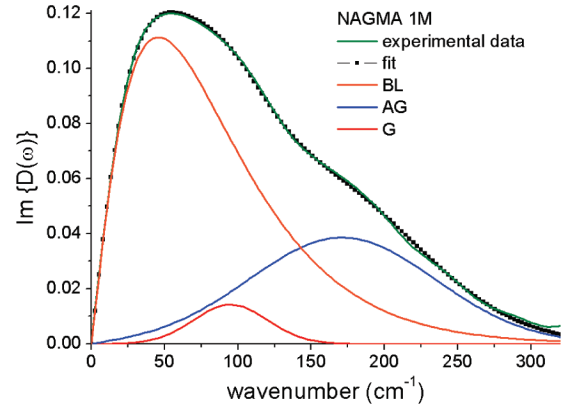

Figure 4. Im $D'(\omega)$ of NAGMA at 1 M fit to the three functions described; BL, ASG, and G denote Bucaro-Litovitz, antisymmetrized Gaussian, and Gaussian, respectively. The green line is the data and the black points the sum of the three fitting functions.

are concentration dependent, relaxing on time scales between tens of femtoseconds and tens of picoseconds. For the first 200 fs the relaxation is characterized by a rapid decay which is oscillatory for both pure water and solutions of low (<0.4 M) peptide concentration. At higher concentrations the oscillatory response is overdamped, i.e., the relaxation time is faster than the inverse of the oscillation frequency, so no oscillation is resolved. However, at concentrations above 0.4 M a new oscillatory feature appears peaking at ca. 500 fs. Beyond 1 ps the relaxation is characterized by a monotonic but nonsingle-exponential relaxation. As the concentration increases, this relaxation time becomes longer, an effect that is particularly evident at concentrations above 1.0 M, where the slowest part of the relaxation has components of up to 20 ps.

It is evident from Figure 2 that the $S(t)$ has two components, a subpicosecond under- or overdamped oscillatory response followed by a component relaxing on the picosecond time scale. On transformation to the frequency domain the latter contributes a narrow intense signal near zero frequency. For water and aqueous solutions the spectroscopically most interesting data, associated with the H-bonding structure, are found at higher frequencies.[31−36] Thus, prior to FT analysis the slowly relaxing picosecond part of $S(t)$ is subtracted from the data to highlight the THz frequency range;[22,23] to indicate this fact the result is called the reduced RSD, $D'(\omega)$. In addition, only the imaginary part of the FT is retained to remove the contribution of the symmetrical electronic response, yielding finally Im $D'(\omega)$; the results for NAGMA are shown in Figure 3. Evidently there is considerable evolution in the shape of Im $D'(\omega)$; with increasing concentration of NAGMA the well-resolved bimodal profile characteristic of pure water[31,37−39] collapses to a single band with a complex profile and a lower mean frequency than pure water.

The Im $D'(\omega)$ can all be fit by a sum of three line shape functions: an antisymmetrized Gaussian represents the highest frequency component

$$I_{\mathrm{ASG}} \propto \exp(-\omega_-^2) - \exp(-\omega_+^2)$$

in which $\omega_\pm = [(\omega \pm \omega_{\mathrm{ASG}})/\Delta\omega_{\mathrm{ASG}})]$, ω_{ASG} is the central frequency, and $\Delta\omega_{\mathrm{ASG}}$ is the full width at half-maximum of each Gaussian composing the ASG function; the intermediate frequency contribution is fit by a simple Gaussian (which is only required at higher peptide concentration, see below) and is characterized by a central frequency ω_{G} and a width $\Delta\omega_{\mathrm{G}}$; at low frequency a Bucaro-Litovitz (or generalized Ohmic) line shape is used[40]

$$I_{\mathrm{BL}} \propto \omega^{\alpha}\exp[-(\omega/\omega_{\mathrm{BL}})]$$

in which ω_{BL} is a characteristic frequency and α a fitting parameter. This procedure results in a good fit to the RSD (Figure 4); further details of the analysis are given in Supporting Information

Raman Spectral Density and H-bond Structure. The bimodal structure of Im $D'(\omega)$ for pure liquid water (Figure 3) has been studied in detail by a number of groups.[31,37,38,41] The lower and higher frequency bands are assigned to restricted translational modes. Specifically, the lower frequency mode is assigned to H-bond bending and the higher to H-bond stretching (although the role of H bonding in the lower frequency part has been a matter of discussion[42−44]). At higher frequencies there is a third, less intense, band assigned to water librational dynamics.[31] These assignments have their origins in the early work of Walrafen, who related them to tetrahedral order in water,[45,46] but they are still a matter of debate. Molecular dynamics simulations showed that the low-frequency bands are well described by hindered translational modes.[43] Padro and Marti[47] carried out molecular dynamics simulations for light and heavy alcohols and found that the low-frequency band (around 60 cm^{-1}) is present even for liquids which do not present hydrogen bonding. On the other hand, the high-frequency band (around 180 cm^{-1}) is only present when there is structure due to hydrogen bonding. This was corroborated by the measurements of De Santis et al.,[48] who measured the Raman spectrum of H_2S, which has similar properties to water but does not form hydrogen bonds; the band around 180 cm^{-1} is absent in H_2S, but no differences were seen in the low-frequency region. Further support to these assignments comes from OKE and dynamic light scattering experiments.[41,49,50] Vohringer presented a detailed line shape analysis of the OHD-OKE spectra of water and concluded that they indicated an inhomogeneous distribution of H-bonded aggregates interconverting on a subpicosecond time scale.[31]

Thus, the Im $D'(\omega)$ line shape is expected to be a sensitive function of the H-bonding structure in solution. The evolution of the spectrum with increasing NAGMA concentration is shown in Figure 3. In Figure 5 the mean frequencies, $\langle\omega\rangle = \int\omega I(\omega)d\omega/\int I(\omega)d\omega$, and relative weights of the three-component fit to the Im $D'(\omega)$ are shown for all three peptides studied. Below 0.4

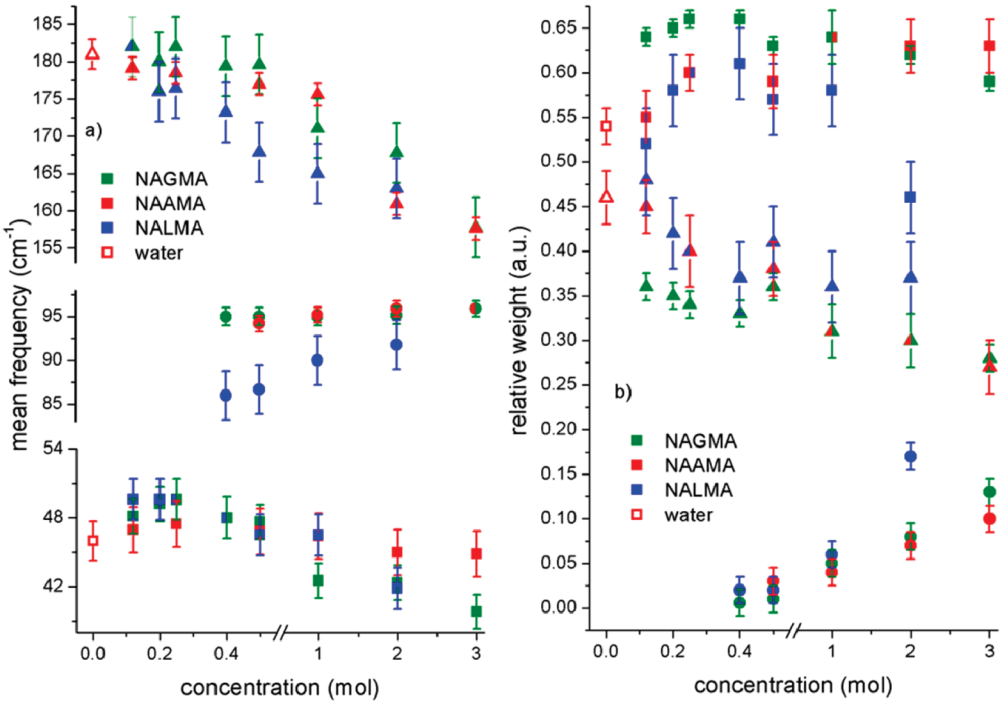

Figure 5. (a) Mean frequency and (b) relative weight of spectral components for the three peptides studied. Square, dot, and triangle denote Bucaro-Litovitz, Gaussian, and antisymmetrized Gaussian functions, respectively.

M the bimodal structure characteristic of pure water is retained, and the weight of the intermediate Gaussian component is negligible. The most significant effect of increasing peptide concentration in this range is a small decrease in the relative amplitude of the higher frequency (H-bond stretching) mode (Figures 3 and 5). This is consistent with a minor change in the fraction of linear H bonds. These data suggest that the overall tetrahedral water structure is largely maintained at these low concentrations, where there are in excess of 100 water molecules per peptide.

As the peptide concentration increases beyond 0.4 M there is a more marked change in the Im $D'(\omega)$ (Figures 3 and 5). Essentially the bimodal profile collapses to an asymmetric band with a reduced mean frequency. A similar evolution in line shape is observed in this concentration range for aqueous electrolyte solutions.[33,51] Analysis (Figure 5) shows that the main changes are a decrease in both the relative weight and frequency of I_{ASG}, indicating disruption of the H-bond structure, and a growth in amplitude of the intermediate Gaussian mode at ca. 90 cm^{-1}, which has a zero weight at concentrations below 0.4 M. There are only small changes in the frequency and relative weight of the low-frequency I_{BL} line shape function. The behavior is quite similar for all three peptides studied. However, the changes in I_{ASG} occur at a slightly lower mole fraction for the amphiphilic NALMA than for NAGMA and NAAMA. This may reflect the greater physical size of NALMA, causing it to perturb more water molecules than the smaller peptides. We calculate the number of water molecules in the first solvation shell of a single peptide molecule on the basis of the relative area of peptide and water molecules and thus obtain 43, 38, and 32 waters surrounding NALMA, NAAMA, and NAGMA, respectively. In MD simulations NALMA and NAGMA were calculated to have 43 and 33 water molecules, respectively, in the first solvation shell, in good agreement with these simple geometric arguments.[19]

The evolution of the high-frequency I_{ASG} component observed here is consistent with a decrease in tetrahedral order in the aqueous solution with increasing peptide concentration.[52] It is significant that the attenuation and red shift in ω_{ASG} become particularly marked only at concentrations between 0.5 and 1 M. At 1 M there are only just sufficient water molecules to provide one complete solvation shell for NALMA. As a consequence of this water molecules which have a peptide as nearest neighbor are on average more likely to be H bonded to a water molecule surrounding another (or the same) peptide rather than to a 'bulk' water molecule. Thus, a plausible interpretation of the data in Figure 5 is that the absence of such bulk water molecules at higher concentrations leads to a significant change in the ability of water molecules to occupy the tetrahedral sites characteristic of pure water (and lower peptide concentrations).

Gaussian Mode. The 90 cm^{-1} mode fit by the Gaussian component can be shown (Figure S2, Supporting Information) by an inverse FT to be responsible for the oscillation peaking around 500 fs in the $S(t)$ measured at higher peptide concentrations (Figure 2). Its growth in amplitude as a linear function of concentration suggests an assignment to a peptide mode (Figure 5). A similar mode has been widely reported in OHD-OKE and low-frequency Raman scattering studies of a range of peptides, amides, and proteins.[53−55] The linear dependence (over the limited concentration range studied) suggests a mode associated with a peptide monomer. There is convincing evidence for the existence of cyclic dimers and chain-like aggregates for model peptides[56] in aqueous solution, and these support low-frequency modes. However, such aggregates cannot be formed by NALMA for steric reasons, yet the mode is certainly not suppressed in that case (Figure 5). Consequently, this mode is more likely to be associated with a solvated peptide monomer.

To investigate further the origin of this mode we conducted OHD-OKE measurements on formamide (FA) and dimethyl FA (DMF) (Figure S3 and Table S1, Supporting Information) and performed DFT calculations on these model compounds as well as on the peptides NAGMA and NAAMA with one or two added water molecules (the results are summarized in Figure

S5, Supporting Information). A strong Gaussian feature was observed in the Im $D'(\omega)$ of the H-bonding liquid FA (96 cm^{-1}) but not in DMF. Two other groups employed OHD-OKE to study the related molecules *N*-methylformamide (NMF),[53] acetamide (Ac),[57] and *N*-methylacetamide (NMA);[57] they found modes at 109, 100, and 80 cm^{-1}, respectively. The NMF mode was assigned to H-bond interactions, whereas for Ac and NMA these modes were characterized as librational bands. No corresponding low-frequency intramolecular modes were found in DFT calculations on the isolated amides. Together these data support the idea that this mode arises from either molecular libration or an H-bonded complex of the amides.[53,54] Significantly, the Gaussian mode persists in aqueous solutions of FA even down to a concentration of 1 M (although it shifts to lower frequency by 15 cm^{-1}, see Supporting Information). This suggests that the mode arises through FA−water as well as FA−FA interactions. On the basis of the MD calculations of Elola and Ladanyi this feature may be assigned to librational modes of FA in the H-bonded complex. However, molecular librations of a dipeptide will occur at a much lower frequency because of the larger moment of inertia; however, a wealth of new low-frequency intramolecular modes will be available in these more flexible solutes. The DFT calculations on dipeptides revealed a number of such low-frequency modes but did not detect any specific intense Raman active mode at around 90−100 cm^{-1}. One or two added water molecules significantly perturbed and enhanced the calculated low-frequency Raman spectra (see Supporting Information), as also reported by Shirota and Ushiyama,[34] but again no unique mode was observed to which the 90 cm^{-1} component could be assigned. It seems likely therefore that the Gaussian component is associated with vibrational motion in an H-bonded solvated peptide. Although the present data do not allow a definitive assignment, all of the plausible assignments support an intermolecular origin and a role for solvent−solute H-bonded interactions in this mode.

Picosecond Molecular Dynamics. The picosecond dynamics of pure water observed in OHD-OKE and low-frequency Raman scattering measurements have been analyzed in considerable detail.[25,31,38,58] In contrast to the $S(t)$ measured for many molecular liquids,[22] the picosecond dynamics in water cannot be assigned to molecular orientational relaxation because the polarizability of water is approximately isotropic,[59] so reorientation does not modify the polarizability. Instead, the measured dynamics reflect translational and rotational−translational interaction-induced (intermolecular) dynamics. Specifically, it has been suggested on the basis of both experiment and simulation that picosecond dynamics in $R(t)$ for liquid water reflects a local structural reorganization of the water H-bonded network.[31,32,52,58] Thus, the dynamics observed in $R(t)$ reflect quite different molecular motions compared with the orientational dynamics observed in NMR and dielectric relaxation measurements. However, translational dynamics related to those seen in OHD-OKE may also contribute to neutron scattering measurements.[16]

The functional form of the picosecond OHD-OKE relaxation for pure water has also been discussed elsewhere.[60] All measurements agree that the picosecond component of $R(t)$ is nonexponential but can be fit either by a sum of two exponentials[31,50,60] (suggesting a biexponential $\psi_{xz}(t)$) or by assuming a correlation function represented by a stretched exponential (Kohlrauch−William−Watts) function: $\psi_{xz}(t) \propto \exp(-t/\tau)^{\beta}$, in which case[58,61]

$$R(t) \propto \frac{\beta t^{\beta-1}}{\tau^{\beta}} \exp\left[-\left(\frac{t}{\tau}\right)^{\beta}\right]$$

TABLE 1: Fit Parameters of the Picosecond Time-Domain Data Obtained for Representative NAGMA and NALMA Solutions[a]

	NAGMA		NALMA	
concentration/mol	β	τ /ps	β	τ /ps
0.0	0.56	0.35	0.56	0.35
0.5	0.51	1.92	0.51	1.75
2	0.55	14.55	0.52	7.33

[a] For full details see the Supporting Information.

We have fit all $S(t)$ data for the three peptides from 600 fs up to the time at which the signal could not be distinguished from background. Both the biexponential and stretched exponential forms provided adequate fits to the data, but in all cases the stretched exponential yielded the better description, as indicated by the reduced chi-square value. The fitting parameters recovered at selected concentrations are shown for two peptides in Table 1 and the full details are included in the Supporting Information(Figure S4 and Table S2). No trend in β with concentration was observed, and for all peptides the β value was approximately constant with a mean value of 0.54. For subsequent analysis we report the mean relaxation time associated with $\psi_{xz}(t)$, given by $\langle\tau\rangle = (\tau/\beta)\Gamma(1/\beta)$, where $\Gamma(x)$ is the gamma function.

In Figure 6 $\langle\tau\rangle$ for all three peptides are plotted as a function of concentration and (for NAGMA and NALMA) the dependence on solution viscosity is shown, where the viscosity is itself a function of concentration. These data show that for all three peptide solutions the structural reorganization reflected in the $S(t)$ is slower than in pure liquid water. As found for the RSD, there are two distinct concentration regions (Figure 6a). At low concentration $\langle\tau\rangle$ increases slowly with increasing concentration and extrapolates back to the bulk water value. Above 0.4 M the effect of increasing concentration is larger and the relaxation slows dramatically, such that for 3 M NAGMA the measured relaxation is up to 30 times slower than in bulk water. However, at these very high concentrations relaxation processes associated with the peptide also contribute to $S(t)$. These two concentration regions will be analyzed separately below.

Even without a quantitative analysis it is apparent in Figure 6 that the slow down in structural reorganization with increasing peptide concentration is a more significant effect for the hydrophilic NAGMA than for the amphiphilic NALMA, which persistently has the faster relaxation time. This is consistent with hydrophilic interactions leading to slower structural dynamics in aqueous peptide solutions than do hydrophobic interactions.[16,18] Significantly, in contrast to the relaxation dynamics, NALMA causes a small but consistently greater increase in solution viscosity than NAGMA at the same concentration (Figure 6c). Although the concentration dependence of the viscosity of peptide solutions is in general complex, this result does confirm that the structural relaxation probed by OHD-OKE is not sensitive to bulk viscosity in the way that might be predicted for orientational relaxation, through the Stokes−Einstein−Debye relation, for example. It is difficult to account for the dependence of solution viscosity on peptide concentration with any certainty, but the different behavior of NALMA and NAGMA may simply reflect the greater volume fraction occupied by the former at any given concentration (e.g., 0.23 and 0.17 for NALMA and NAGMA, respectively, at 2 M concentration). Such behavior would be consistent with the simple Einstein relation linking viscosity to a volume fraction

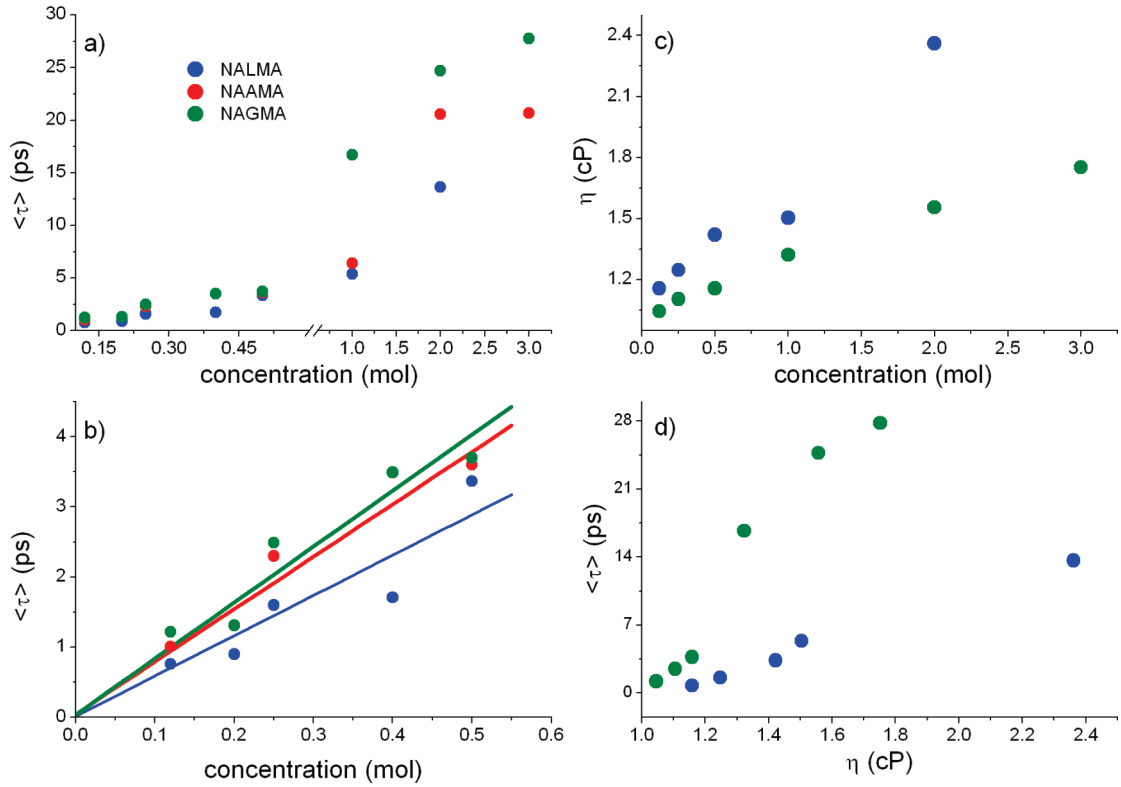

Figure 6. (a) Dependence of $\langle\tau\rangle$ on concentration for all three peptides. (b) Fit to the two-population analysis at low concentration. (c) Solution viscosity as a function of concentration. (d) Correlation of $\langle\tau\rangle$ with viscosity.

of (noninteracting) spheres in solution (although it seems unlikely that the underlying assumptions of the Einstein relation will be met at the microscopic level by peptides in water).

To analyze quantitatively the effect of peptide on the picosecond structural dynamics in liquid water at low concentration (<0.5 M) we adopt a two-state model and apply it to the picosecond time scale $S(t)$ data. Similar models have been applied to analyze NMR relaxation times in peptide solutions[19] and to model the low-frequency Raman scattering of glucose solutions.[52] Here two assumptions are made: first, that the concentration-dependent $\langle\tau\rangle$ reflects an average of the relaxation times associated with two populations, solvation water (WS) and free or bulk like water (WF), weighted by their mole fractions, X_i

$$\langle\tau\rangle = X_{WS}\tau_{WS} + X_{WF}\tau_{WF}$$

and, second, that both components contribute equally to the amplitude of the RSD. In that case the equation may be rewritten in the linear form

$$\langle\tau\rangle = \left(\frac{n_P}{n_W}\right)n_S(\tau_{WS} - \tau_{WF}) + \tau_{WF}$$

in which (n_P/n_W) is the molar ratio of peptide to water and n_S is the number of water molecules solvating the peptide. A plot of $\langle\tau\rangle$ against (n_P/n_W) thus yields the product of n_S and the difference in the relaxation times $(\tau_{WS} - \tau_{WF})$. The plots are shown in Figure 6b. The linear relation holds up to at least 0.4 M, and significantly, the data extrapolate back to the relaxation time of bulk water. If the n_S values calculated earlier for NAGMA and NALMA using geometric arguments are assumed (along with the value calculated for NAAMA, 38) the relaxation times, τ_{WS}, obtained are 12.4 ps for NAGMA, 9.7 ps for NAAMA, and 7.2 ps for NALMA. Again, the result is consistent with a greater slowing down of the structural relaxation in water due to the hydrophilic solutes rather than the amphiphilic solute NALMA. This result is in turn consistent with recent molecular dynamics studies of H-bonding lifetimes for amphiphilic solutes and amino acids.[62,63]

The relaxation times recovered from the analysis are significantly longer than those reported in NMR relaxation experiments. Since NMR and OHD-OKE probe quite different dynamics, a correspondence is not expected. However, two factors should be noted which could contribute to the recovery of an artificially long relaxation time from the two-state analysis of $S(t)$. First, the long relaxation times are indicative of a strong effect of the peptide on the relaxation dynamics even at low concentration. It is possible that at the very lowest concentrations the solute influences the structural reorganization measured by OHD-OKE in water molecules beyond the first solvation shell. In that case the relaxation time is overestimated (or, equivalently, n_S underestimated). Such long-range effects of proteins and peptides on the structure and dynamics of solvation water have been reported on the basis of THz transmission spectra.[6] There is also evidence for peptide solvation layers extending beyond the first solvation shell in incoherent quasi-elastic neutron scattering.[17] Second, if the depolarized Raman cross section for the WS population is larger than that for WF this will tend to weight the $\langle\tau\rangle$ toward longer times, even if the solute effect is restricted to the first solvation shell. Additional experiments are required to separate these two possibilities.

At peptide concentrations above 0.5 M the measured relaxation time slows appreciably and the data no longer extrapolate to the bulk water relaxation time at low concentration. This slow down occurs when the number of solvent molecules is sufficient

for at most two complete solvation shells and at the highest concentrations less than one complete solvation shell per solute. Significantly, it also correlates with a substantial disruption of the tetrahedral order characteristic of bulk water (Figure 3). The extended relaxation time observed here is also consistent with the strong nonlinear concentration dependence reported in THz transmission spectroscopy[6] and with observations of slow dynamics in dielectric relaxation at high concentrations.[20]

At the higher peptide concentration both the solute and the solvent can contribute to the measured $S(t)$. The solute could in principle contribute a slow component due to orientational relaxation. However, the degree of pump-induced alignment of a relatively massive peptide molecule will be small for the low-intensity pulses used here, making any such effect a minor component of the relaxation. Further, the size of the solutes and the viscosity of the solution means that the calculated reorientation time (e.g., by the Stokes−Einstein−Debye equation) is longer than the tens of picosecond relaxation observed here. Very low-frequency intramolecular modes of the peptide (such as torsional reorganization) may contribute to the observed relaxation, but such modes will themselves be strongly coupled to the solvent dynamics, since they reflect the solvent friction,[64] and solvent molecules must reorganize to accommodate them. Finally, the crowding of the solvation layer between adjacent solute molecules may itself contribute to a slowing down of structural reorganization within the solvating water molecules. One such mechanism has been highlighted in the simulations of Hynes, Laage, and co-workers.[63] H-bond reorganization in the solvation layer requires the approach of a free water molecule to form a partner for H-bond exchange. As the solute mole fraction increases, the solute may block the approach of the incoming water molecule required. This excluded volume mechanism operates in addition to the slow down due to the hydrophilic site interaction.[63] The appearance of such a restricted geometry at high solute concentration is expected to correlate with the attenuation of the signal due to tetrahedral structure in water in the Im $D'(\omega)$, as observed (Figure 3).

Conclusion

Real-time OHD-OKE measurements of molecular dynamics in peptide solutions reveal a correlation between the degree of tetrahedral structure in the solution and picosecond structural dynamics. The experiments reveal two distinct concentration regimes. At concentrations below 0.4 M, where on average less than 40% of water molecules have a peptide as nearest neighbor, the tetrahedral structure of water is largely preserved. The measured relaxation times in the peptide solution are slower than in bulk water at these low peptide concentrations and increase linearly up to a concentration of 0.4 M. Slower dynamics are observed for the more hydrophilic peptides. The current measurements cannot deconvolute the observed relaxation time from the number of solvating water molecules involved but are consistent with the effect of the peptide on the molecular dynamics extending beyond the first solvation shell. At higher peptide concentration the tetrahedral water structure is perturbed and the measured dynamics are up to 30 times slower than in bulk water. In this case the observed dynamics are not a property of the water alone but reflect relaxation in the H-bonded network of solvated peptide molecules. This change in the nature of the relaxation mechanism highlights the importance of concentration-dependent experiments when measuring relaxations in aqueous peptide solutions.

Acknowledgment. We are grateful to the EPSRC for financial support (EP/E010466/1). K.M. thanks the University of East Anglia for the award of a studentship.

Supporting Information Available: Additional information is presented including: figures similar to those in the main text for NAGMA for NALMA and NAAMA; details of time- and frequency-domain analysis; fit parameters for all data sets; DFT calculations. This material is available free of charge via the Internet at http://pubs.acs.org.

References and Notes

(1) Ball, P. *Chem. Rev.* **2008**, *108*, 74.
(2) Papoian, G. A.; Ulander, J.; Eastwood, M. P.; Luthey-Schulten, Z.; Wolynes, P. G. *Proc. Natl. Acad. Sci. U.S.A.* **2004**, *101*, 3352.
(3) Helms, V. *ChemPhysChem* **2007**, *8*, 23.
(4) Sorenson, J. M.; Hura, G.; Soper, A. K.; Pertsemlidis, A.; Head-Gordon, T. *J. Phys. Chem. B* **1999**, *103*, 5413.
(5) Khodadadi, S.; Pawlus, S.; Sokolov, A. P. *J. Phys. Chem. B* **2008**, *112*, 14273.
(6) Heugen, U.; Schwaab, G.; Brundermann, E.; Heyden, M.; Yu, X.; Leitner, D. M.; Havenith, M. *Proc. Natl. Acad. Sci. U.S.A.* **2006**, *103*, 12301.
(7) Shenogina, N.; Keblinski, P.; Garde, S. *J. Chem. Phys.* **2008**, *129*, 155105.
(8) Halle, B. *Philos. Trans. R. Soc. London, Ser. B: Biol. Sci.* **2004**, *359*, 1207.
(9) Oleinikova, A.; Sasisanker, P.; Weingartner, H. *J. Phys. Chem. B* **2004**, *108*, 8467.
(10) Qvist, J.; Halle, B. *J. Am. Chem. Soc.* **2008**, *130*, 10345.
(11) Born, B.; Weingartner, H.; Brundermann, E.; Havenith, M. *J. Am. Chem. Soc.* **2009**, *131*, 3752.
(12) Hura, G.; Sorenson, J. M.; Glaeser, R. M.; Head-Gordon, T. *Perspect. Drug Discov.* **1999**, *17*, 97.
(13) Johnson, M. E.; Malardier-Jugroot, C.; Murarka, R. K.; Head-Gordon, T. *J. Phys. Chem. B* **2009**, *113*, 4082.
(14) Sasisanker, P.; Weingartner, H. *ChemPhysChem* **2008**, *9*, 2802.
(15) Malardier-Jugroot, C.; Johnson, M. E.; Murarka, R. K.; Head-Gordon, T. *Phys. Chem. Chem. Phys.* **2008**, *10*, 4903.
(16) Russo, D.; Hura, G.; Head-Gordon, T. *Biophys. J.* **2004**, *86*, 1852.
(17) Russo, D.; Murarka, R. K.; Copley, J. R. D.; Head-Gordon, T. *J. Phys. Chem. B* **2005**, *109*, 12966.
(18) Russo, D.; Murarka, R. K.; Hura, G.; Verschell, E.; Copley, J. R. A.; Head-Gordon, T. *J. Phys. Chem. B* **2004**, *108*, 19885.
(19) Qvist, J.; Persson, E.; Mattea, C.; Halle, B. *Faraday Discuss.* **2009**, *141*, 131.
(20) Murarka, R. K.; Head-Gordon, T. *J. Phys. Chem. B* **2008**, *112*, 179.
(21) Johnson, M. E.; Malardier-Jugroot, C.; Head-Gordon, T. *Phys. Chem. Chem. Phys.* **2010**, *12*, 393.
(22) Hunt, N. T.; Jaye, A. A.; Meech, S. R. *Phys. Chem. Chem. Phys.* **2007**, *9*, 2167.
(23) Zhong, Q.; Fourkas, J. T. *J. Phys. Chem. B* **2008**, *112*, 15529.
(24) Walrafen, G. E. *J. Chem. Phys.* **1964**, *40*, 3249.
(25) Winkler, K.; Lindner, J.; Bursing, H.; Vohringer, P. *J. Chem. Phys.* **2000**, *113*, 4674.
(26) Mizoguchi, K.; Hori, Y.; Tominaga, Y. *J. Chem. Phys.* **1992**, *97*, 1961.
(27) Ladanyi, B. M.; Liang, Y. Q. *J. Chem. Phys.* **1995**, *103*, 6325.
(28) Elola, M. D.; Ladanyi, B. M. *J. Chem. Phys.* **2007**, *126*, 084504.
(29) Lotshaw, W. T.; McMorrow, D.; Thantu, N.; Melinger, J. S.; Kitchenham, R. *J. Raman Spectrosc.* **1995**, *26*, 571.
(30) Watanabe, J.; Tohji, M.; Ohtsuka, E.; Miyake, Y.; Kinoshita, S. *Chem. Phys. Lett.* **2004**, *396*, 232.
(31) Winkler, K.; Lindner, J.; Vohringer, P. *Phys. Chem. Chem. Phys.* **2002**, *4*, 2144.
(32) Ohmine, I.; Saito, S. *Acc. Chem. Res.* **1999**, *32*, 741.
(33) Heisler, I. A.; Meech, S. R. *Science* **2010**, *327*, 857.
(34) Shirota, H.; Ushiyama, H. *J. Phys. Chem. B* **2008**, *112*, 13542.
(35) Chang, Y. J.; Castner, E. W. *J. Phys. Chem.* **1994**, *98*, 9712.
(36) Lerbret, A.; Affouard, F.; Bordat, P.; Hedoux, A.; Guinet, Y.; Descamps, M. *J. Chem. Phys.* **2009**, *131*, 245103.
(37) Walrafen, G. E.; Chu, Y. C.; Piermarini, G. J. *J. Chem. Phys.* **1996**, *100*, 10363.
(38) Palese, S.; Mukamel, S.; Miller, R. J. D.; Lotshaw, W. T. *J. Phys. Chem.* **1996**, *100*, 10380.
(39) Fecko, C. J.; Eaves, J. D.; Tokmakoff, A. *J. Chem. Phys.* **2002**, *117*, 1139.
(40) Bucaro, J. A.; Litovitz, T. A. *J. Chem. Phys.* **1971**, *54*, 3846.
(41) Skaf, M. S.; Sonoda, M. T. *Phys. Rev. Lett.* **2005**, *94*, 137802.

(42) Mazzacurati, V.; Nucara, A.; Ricci, M. A.; Ruocco, G.; Signorelli, G. *J. Chem. Phys.* **1990**, *93*, 7767.
(43) Ohmine, I.; Tanaka, H. *Chem. Rev.* **1993**, *93*, 2545.
(44) Marti, J.; Padro, J. A.; Guardia, E. *J. Chem. Phys.* **1996**, *105*, 639.
(45) Walrafen, G. E.; Fisher, M. R.; Hokmabadi, M. S.; Yang, W. H. *J. Chem. Phys.* **1986**, *85*, 6970.
(46) Walrafen, G. E.; Hokmabadi, M. S.; Yang, W. H.; Chu, Y. C.; Monosmith, B. *J. Phys. Chem.* **1989**, *93*, 2909.
(47) Guardia, E.; Marti, J.; Padro, J. A.; Saiz, L.; Komolkin, A. V. *J. Mol. Liq.* **2002**, *96*−*7*, 3.
(48) Desantis, A.; Sampoli, M.; Mazzacurati, V.; Ricci, M. A. *Chem. Phys. Lett.* **1987**, *133*, 381.
(49) Wakker, A. *J. Phys. Chem.* **1988**, *92*, 6436.
(50) Saito, S.; Ohmine, I. *J. Chem. Phys.* **1997**, *106*, 4889.
(51) Mizoguchi, K.; Ujike, T.; Tominaga, Y. *J. Chem. Phys.* **1998**, *109*, 1867.
(52) Paolantoni, M.; Sassi, P.; Morresi, A.; Santini, S. *J. Chem. Phys.* **2007**, *127*, 024504.
(53) Chang, Y. J.; Castner, E. W. *J. Chem. Phys.* **1993**, *99*, 113.
(54) Colaianni, S. E. M.; Nielsen, O. F. *J. Mol. Struct.* **1995**, *347*, 267.
(55) Giraud, G.; Karolin, J.; Wynne, K. *Biophys. J.* **2003**, *85*, 1903.
(56) Nielsen, O. F. *Annu. Rep. Sect. C: Phys. Chem.* **1997**, *93*, 57.
(57) Hunt, N. T.; Turner, A. R.; Tanaka, H.; Wynne, K. *J. Phys. Chem. B* **2007**, *111*, 9634.
(58) Torre, R.; Bartolini, P.; Righini, R. *Nature* **2004**, *428*, 296.
(59) Murphy, W. F. *J. Chem. Phys.* **1977**, *67*, 5877.
(60) Palese, S.; Schilling, L.; Miller, R. J. D.; Staver, P. R.; Lotshaw, W. T. *J. Phys. Chem.* **1994**, *98*, 6308.
(61) Turton, D. A.; Wynne, K. *J. Chem. Phys.* **2009**, *131*, 201101.
(62) Sterpone, F.; Stirnemann, G.; Hynes, J. T.; Laage, D. *J. Phys. Chem. B* **2010**, *114*, 2083.
(63) Stirnemann, G.; Hynes, J. T.; Laage, D. *J. Phys. Chem. B* **2010**, *114*, 3052.
(64) Hunt, N. T.; Meech, S. R. *Chem. Phys. Lett.* **2003**, *378*, 195.

JP106423A